Electronic Supplementary Information

Two-Dimensional Molecular Moiré Superlattices of Tryptophan with Visible Photoluminescence for Photo-activatable CO_2 Sensing and Storage

Ujjala Dey [a] and Arun Chattopadhyay[a,b]*

[a] Department of Chemistry and [b] Centre for Nanotechnology, Indian Institute of Technology Guwahati, Guwahati 781039, India.

***E-mail: arun@iitg.ac.in**

Table of Contents

EXPERIMENTAL SECTION

Materials Used

L and D-tryptophan (trp) were purchased from Sigma-Aldrich and used without further purification. Mili-Q grade water was used for all the experiments. D_2O was purchased from Sigma-Aldrich and used for NMR experiments.

Synthesis of Moiré Superlattices of trp

2 mL of trp (6 mg) solution was sonicated for 30 s to get a clear solution. 200 μL of the trp solution was added to 10 mL of water (resulting in 288 μM concentration) under constant stirring and heating at 80 ºC for 24 h. The dispersion after 24 h was then used for further experiments.

Optical Measurements

Time dependent UV-vis measurements were done using Perkin-Elmer Lambda 362+ where 3 mL of aliquot was collected at different times and absorbance was measured. Photoluminescence (PL) spectra were collected using HORIBA FluoroMax-4 spectrofluorometer where again 3 mL of aliquot was collected at different times to measure the PL spectrum.

Transmission electron microscopic (TEM) analysis and selected area electron diffraction (SAED) analysis

TEM and SAED data were collected after diluting the dispersion (400 μL of aliquot in 600 μL water) and drop casting on a carbon coated copper grid. TEM and SAED were performed using JEOL JEM 2100 F instrument.

Atomic force microscopic (AFM) analysis and measurement of Force-distance curve

AFM images were acquired using Oxford Asylum Research MFP-3D model. Images were acquired in attractive tapping mode. Force-distance curves were measured in contact mode with tip of model AC240TS-R3 (k~2 Nm^{-1} and f = ~73 kHz).

Proton NMR and ESI-MS

Proton nuclear magnetic resonance (NMR) measurements were performed using 600 MHz Bruker ASCEND 600. The experiment was performed as described in 'synthesis of moiré superlattices' where D_2O (Sigma-Aldrich) was used in place of Mili-Q grade water. 600 μL of aliquot was taken at different times to perform the analysis. Electrospray ionization mass spectrometric (ESI-MS) analysis was performed using Agilent Accurate Mass (Q-TOF 6520) spectrometer in ESI positive mode where 1 mL of the aliquot was used for the analysis.

SAED Simulation and Structure Optimisation

The cif date file of L-trp was used for SAED simulation, which was done using ReciPro software. The unit cell, hkl planes and the structure were redrawn from cif file data using vesta. Twisting of the unit cells were performed using Avogadro software.

CO_2 sensing and storage measurements

3 mL of the dispersion obtained after 24 h of reaction was taken in a cuvette. PL emission of the dispersion was recorded first after which it was purged with CO_2 gas using a balloon. The PL emission was recorded after subsequent purging with CO_2. For UV exposed system, the dispersion was irradiated with UV light in the presence of CO_2 for different extent of time. After each exposure in sequence, the PL emission spectrum was recorded. For release study, the system was kept open for 60 min and PL emission was recorded at different intervals of time.

Rate constant for the reaction of tryptophan assembly:

As observed the photoluminescence (PL) intensity of tryptophan (trp) molecules decreased as the reaction progressed. As trp self-assembled the intrinsic fluorescence intensity of trp molecule decreased as the environment around the molecule in the assembly changed. PL intensity of a fluorophore depends on the concentration according to the following equation

$$I_f = kI_0\phi[1-(10^{-\varepsilon lc})] \quad (1)$$

where κ is a constant depending on the instrument, I_0 is the intensity of incident light, ϵ is the molar absorptivity, l is the path length, ϕ is the quantum yield and C is the concentration. At low concentration this equation would transform into following

$$I_f=\kappa I_0\phi[1-(1-\varepsilon lc)] \quad (2)$$

Or, $$I_f= AC \quad (3)$$

where $A= \kappa I_0\phi\varepsilon l$. Since low concentration (288 µM) of trp was taken for the reaction, the PL intensity would be directly proportional to the concentration, according to equation 3 and thus constant A could be calculated after dividing fluorescence intensity for 288 µM trp by its concentration. The plot of 1/(intensity) vs time for the reaction mentioned here resulted in a liner fit thus following 2nd order kinetics.

$$A/(I_f)_t = 1/C_t = 1/C_0 + kt \quad (4)$$

Or $$1/(I_f)_t = 1/(AC_t)= 1/(AC_0) + (k/A)t \quad (5)$$

Where C_t and $(I_f)_t$ are concentration and intensity of fluorescence at time t, k is the rate constant and C_0 is concentration at t = 0 h. Thus, the slope obtained (k/A) following equation 4 gives the rate constant of the reaction after multiplying it with constant A.

For reactions in Fig. 1(f) Fig. S1a and Fig. S1b the rate constants are 1.28 ×10^{-3}, 1.05 ×10^{-3} and 2.33 ×10^{-3} μM^{-1} h^{-1}, respectively. This gives an average rate constant of (1.55 ± 0.68) × 10^{-3} μM^{-1} h^{-1}.

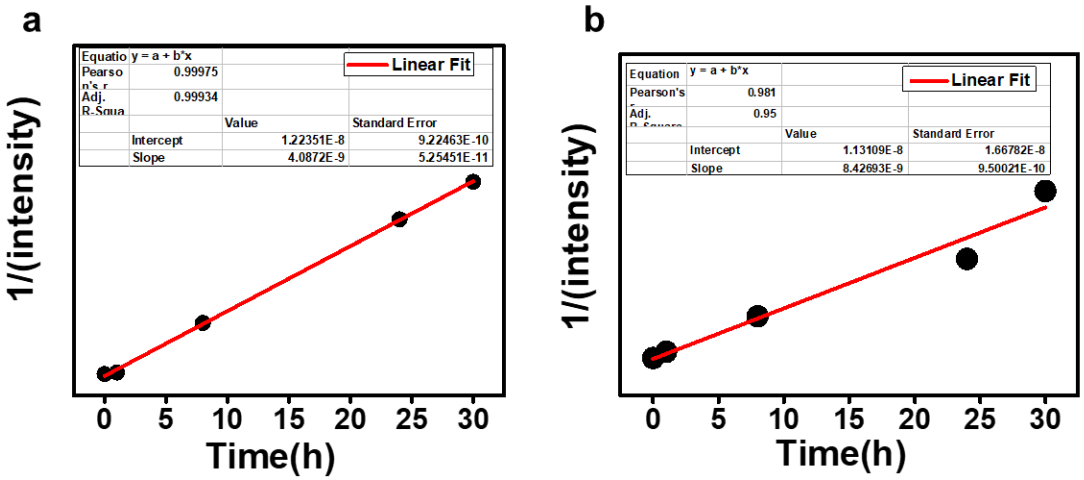

Fig. S1 Rate constant determination. (a) and (b) 1/(intensity) vs time plot for the 360 nm fluorescence peak for two different experimental runs of reaction.

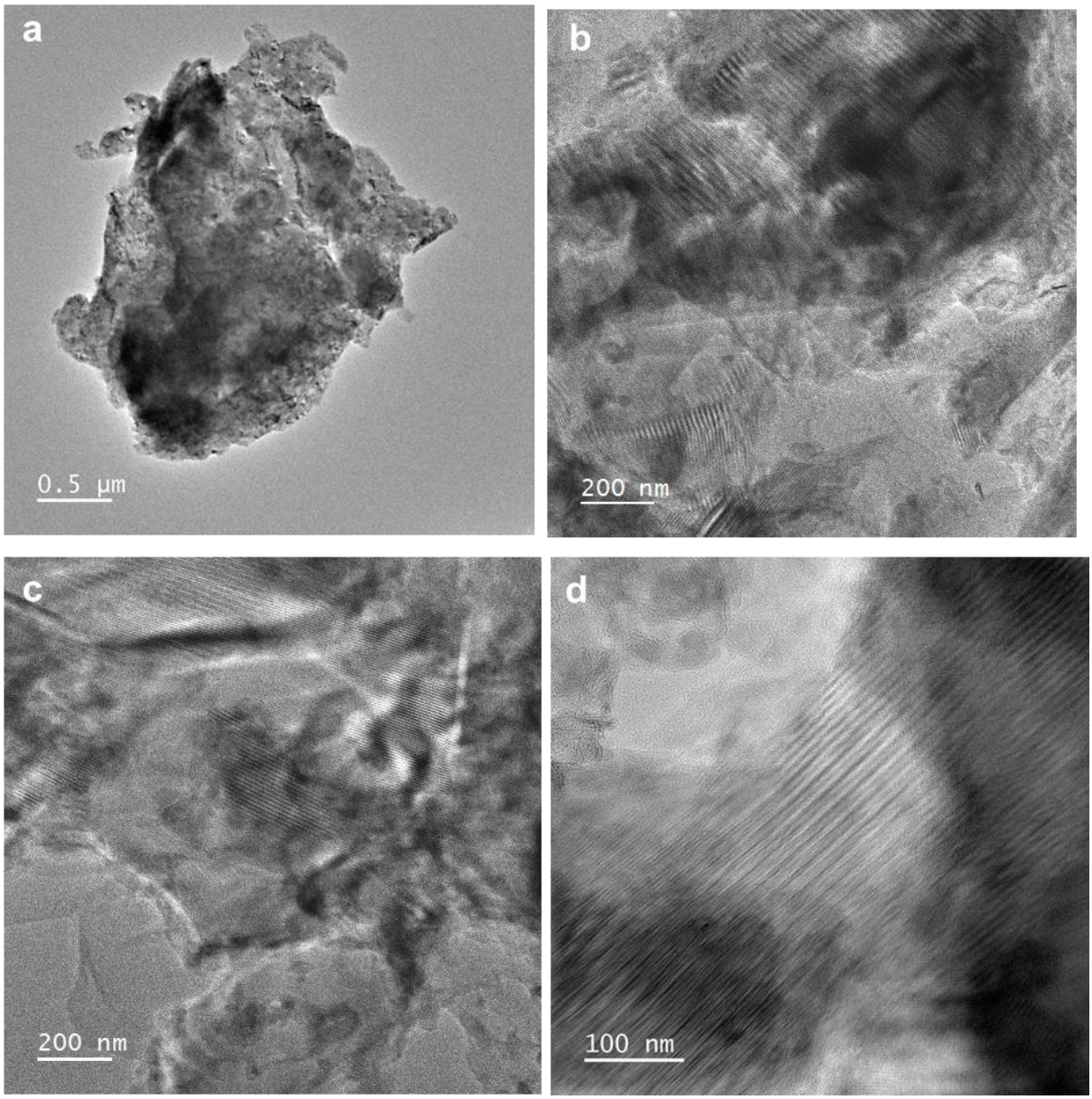

Fig. S2 Transmission emission microscopic (TEM) images of samples at different times. TEM images of the trp dispersion taken at **(a)** 5 min; **(b)** 1 h; **(c)** 8 h and **(d)** 30 h of reaction.

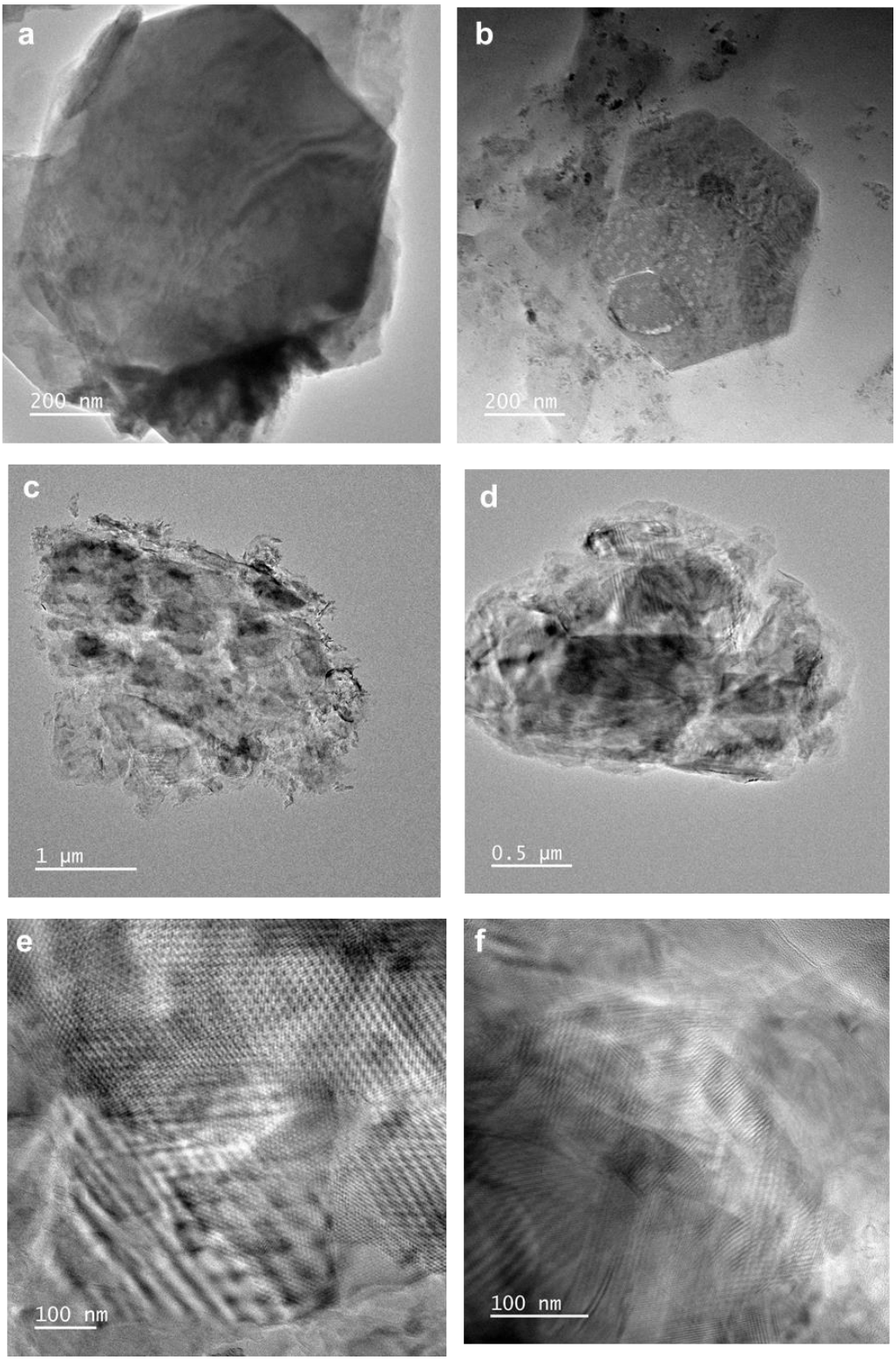

Fig. S3 Transmission microscopic images (TEM) showing nanosheets observed from the dispersion of (**a) and (b)** single crystalline nanosheet of D-trp and L-trp respectively. (**c) and (d)** moiré nanosheet of D-trp and L-trp respectively. (**e) and (f)** enlarged image of (**c)** and **(d)** respectively showing moiré superlattices.

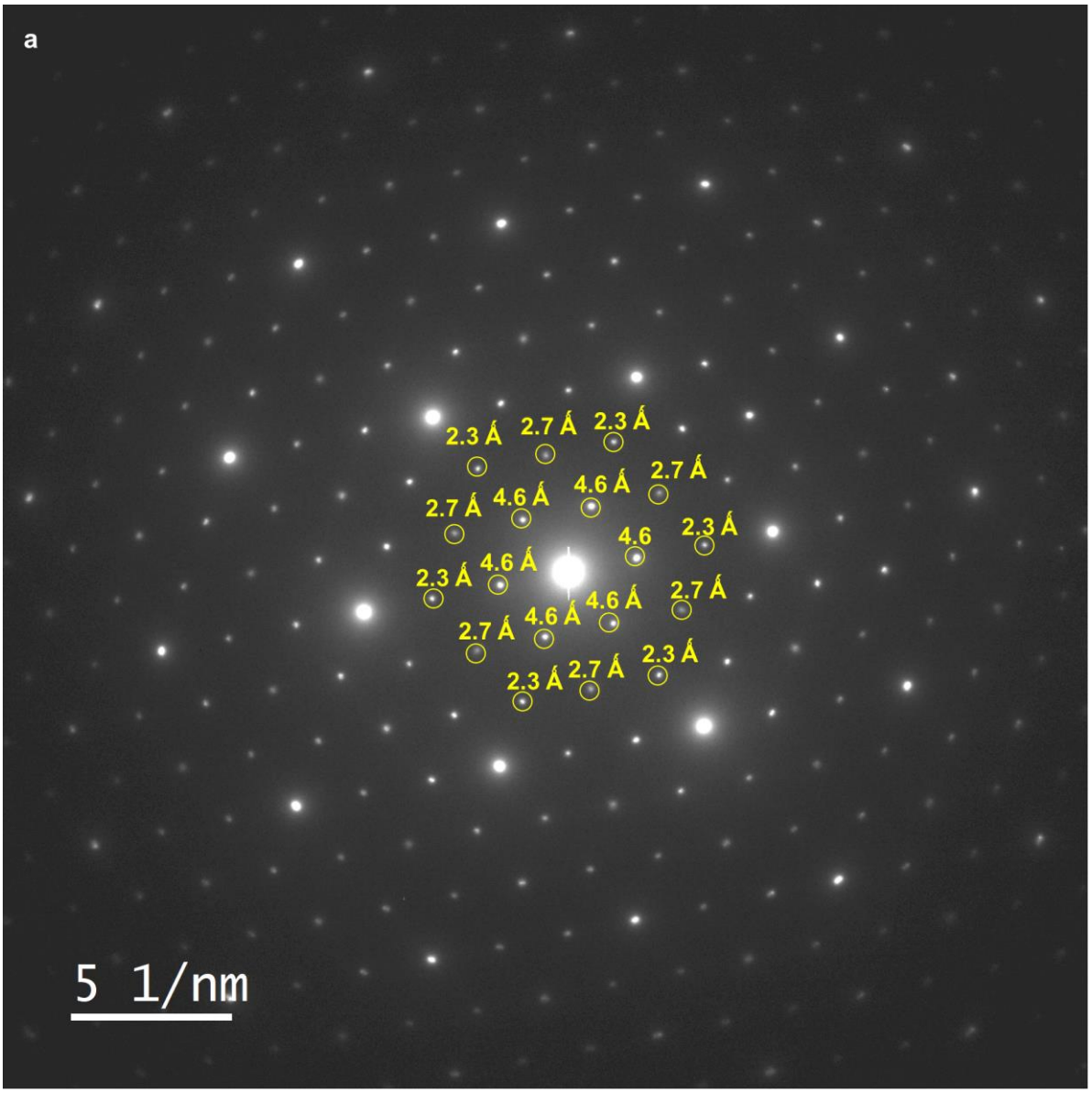

Fig. S4 SAED pattern of the crystalline nanosheet from Fig. 2B with d–spacing as calculated from the central spot.

Table S1. Comparison of experimental and simulated d-spacing

hkl planes	d-spacing (Å) obtained from SAED	Simulated d-spacing (Å) from cif file of trp
020	4.6	4.9
0-20	4.6	4.9
200	4.6	4.9
-200	4.6	4.9
220	4.6	4.9
-2-20	4.6	4.9
420	2.7	2.8
-4-20	2.7	2.8
240	2.7	2.8
-2-40	2.7	2.8
-220	2.7	2.8
2-20	2.7	2.8
040	2.3	2.4
0-40	2.3	2.4
400	2.3	2.4
-400	2.3	2.4
440	2.3	2.4
-4-40	2.3	2.4

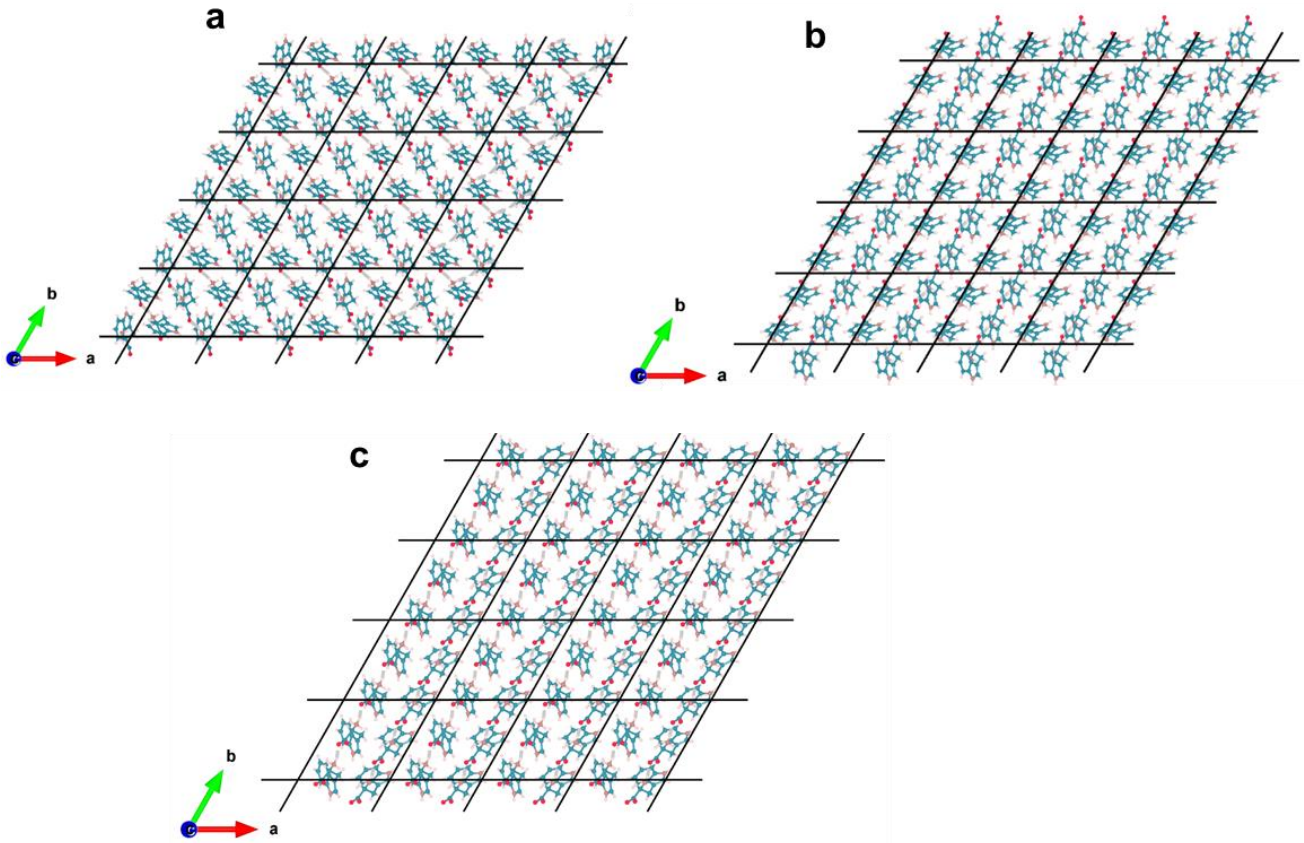

Fig. S5 Subsequent layers of trp (beyond the first layer as depicted in Fig. 2(e) in the self-assembly to form crystalline nanosheet. (a) 2nd layer of the supercell viewed along the

c axis. **(b)** 3rd layer of the supercell viewed along the c axis. **(c)** 4th layer of the supercell viewed along the c axis. The first layer is presented in Fig. 2e.

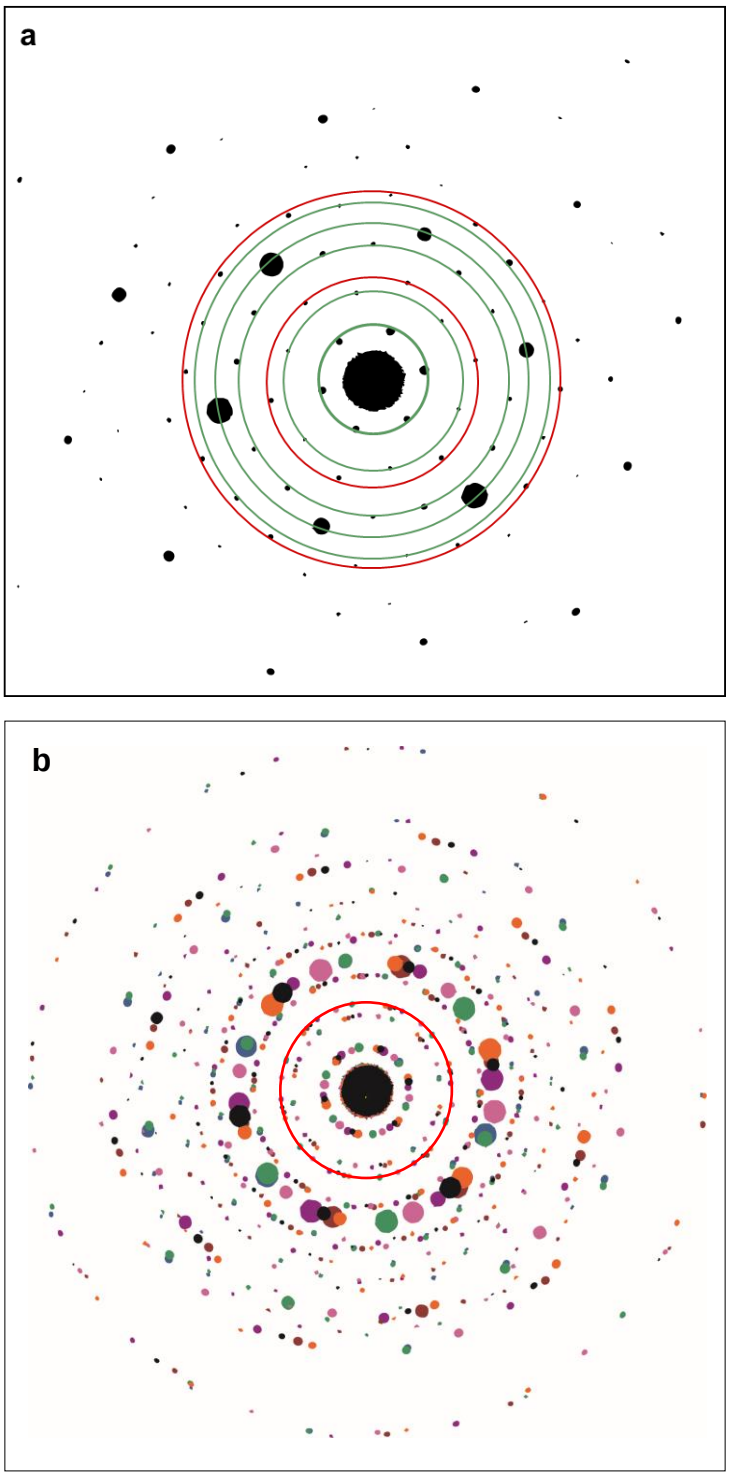

Fig. S6 Superimposition of hexagonal SAED patterns. (a) Crystalline hexagonal SAED patterns where diffraction spots in the red circles were observed in the SAED pattern of moiré superlattices of Fig. 3c and Fig. 3f. **(b)** Superposition of the hexagonal SAED pattern

rotated according to the angles in Table S1 to reproduce the SAED pattern obtained for moiré superlattices.

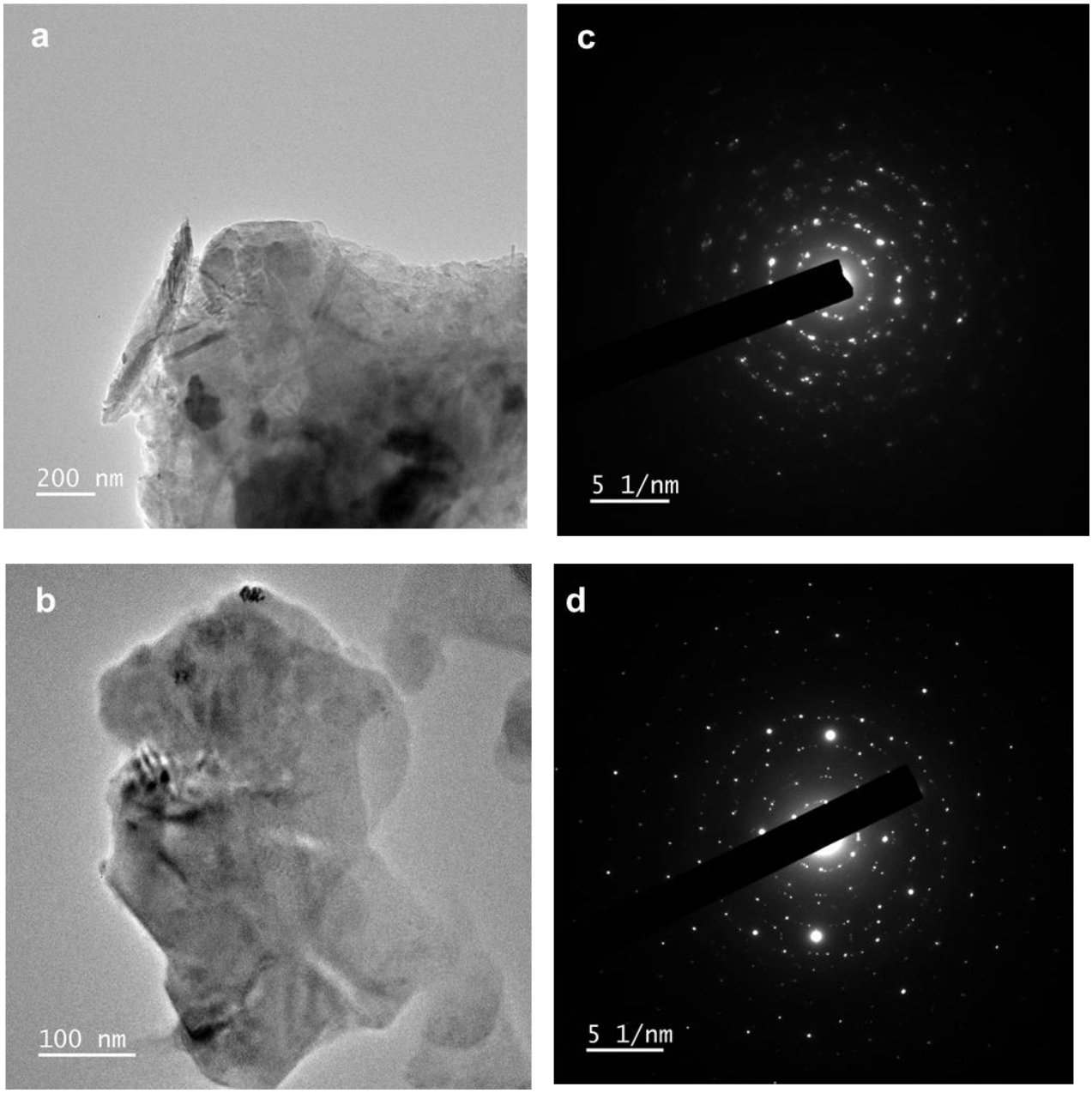

Fig. S7 (a) and (b) Multi-layered sheet formed after twisted stacking of crystalline nanosheets showing no moiré patterns. (**c) and (d)** Corresponding SAED patterns of (**a) and (b)** respectively having d spacing 0.46 nm.

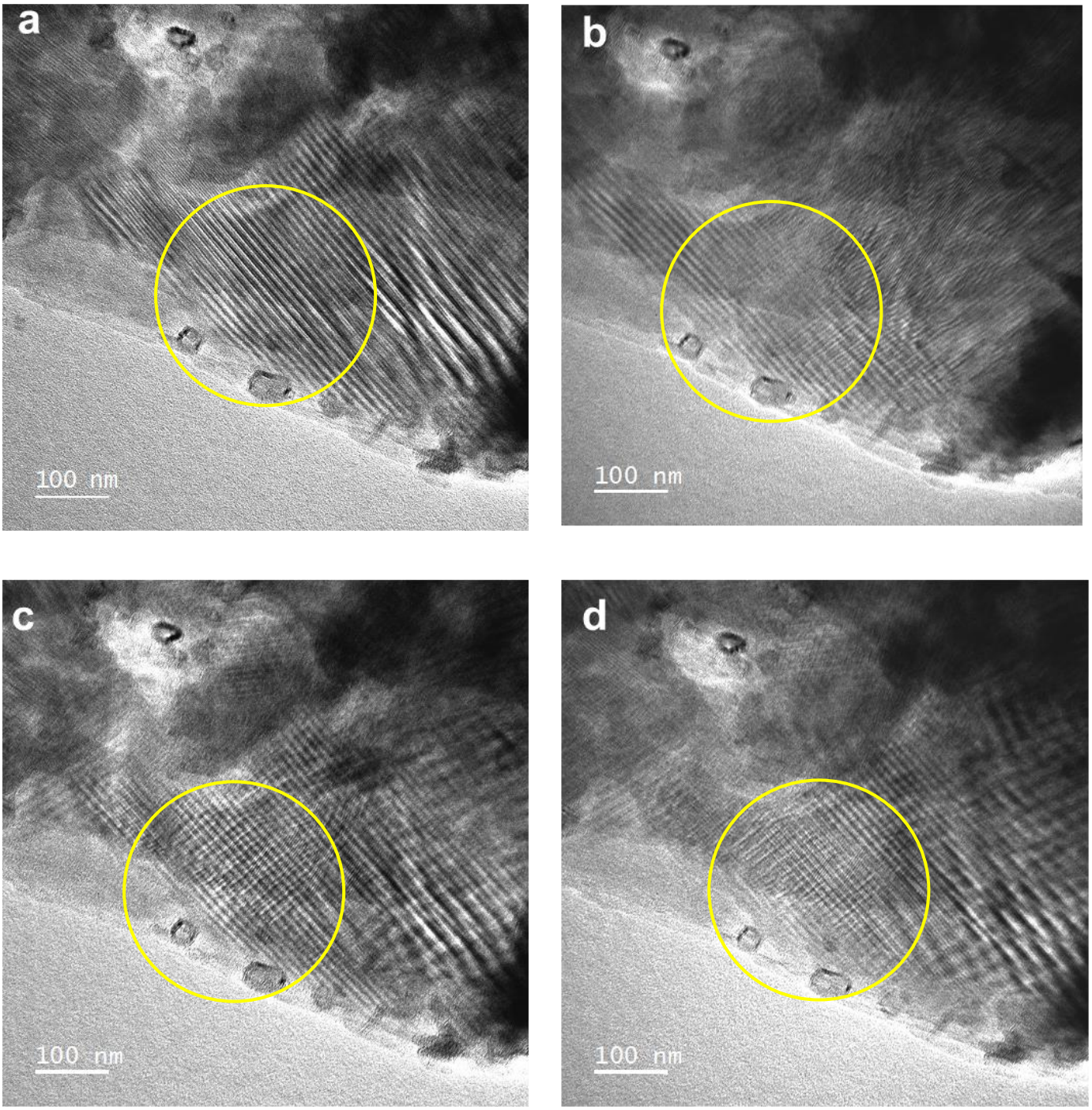

Fig. S8 (a) TEM image of a typical moiré nanosheet with parallel line patterns. The same image recorded following tilting of the specimen along direction **(b)** x = 2º and y = 1º, **(c)** x = 5º and y = 8º, **(d)** x = 4º and y = 8º, respectively. The portions encircled in yellow exhibited the change in moiré patterns from parallel lines to cross patterns as the specimen was tilted accordingly.

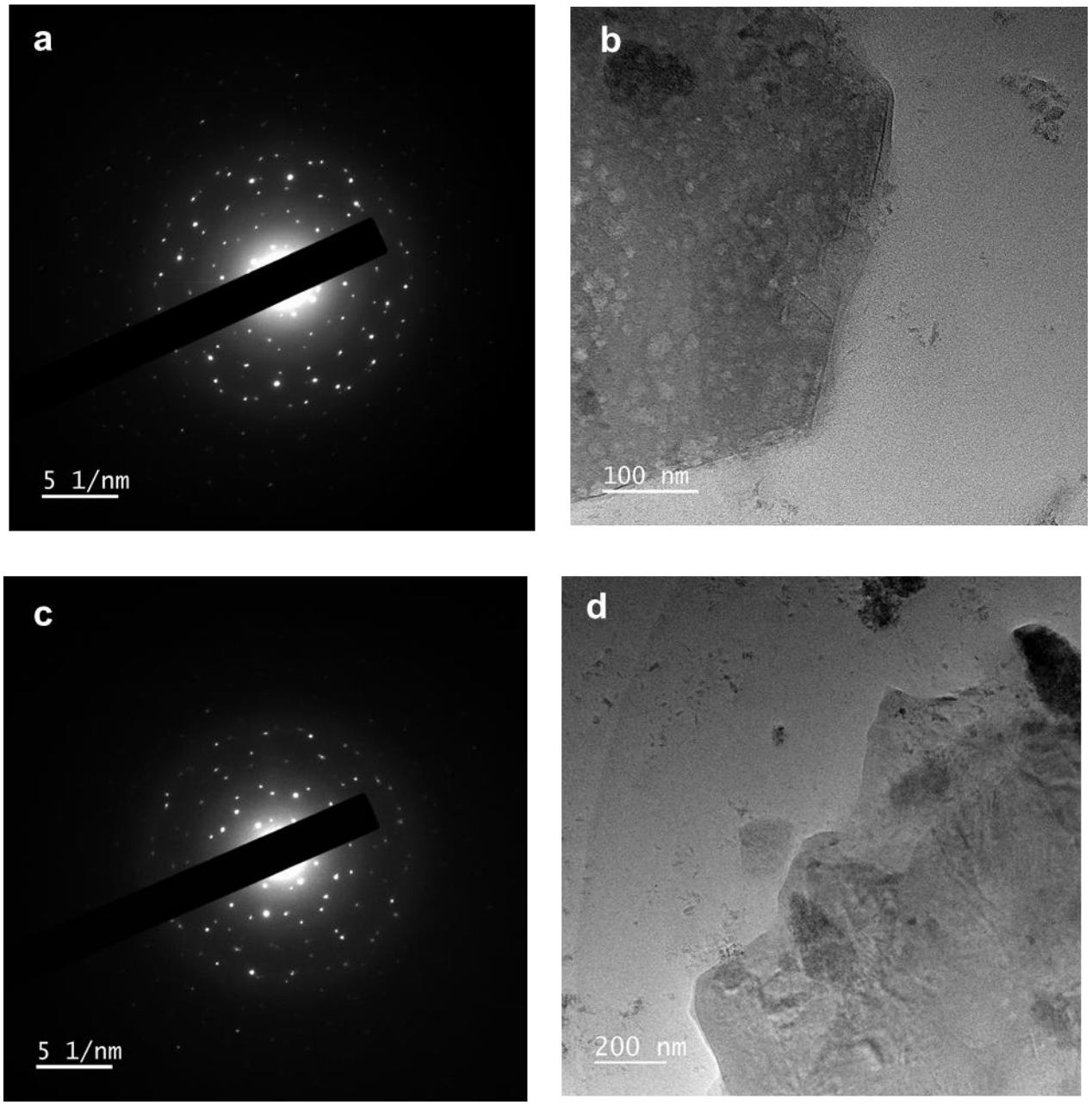

Fig. S9 (a) SAED pattern where two hexagonal patterns superimposed at an angle 25º and **(b)** corresponding TEM images of D-trp nanosheets from where the SAED pattern were acquired. **(c)** SAED pattern where two hexagonal patterns superimposed at an angle 25.6º. **(d)** corresponding TEM images of L-trp nanosheets from where the SAED pattern were acquired.

Table S2. The angles between the adjacent nanosheets after twisted stacking.

sheet number	Rotation of nanosheet with respect to sheet 1	angle with respect to the previous sheet
1	0	-
2	28.9	28.9
3	53.9	25
4	87.6	33.7
5	122.9	35.3
6	159.3	36.4
7	187.2	27.9

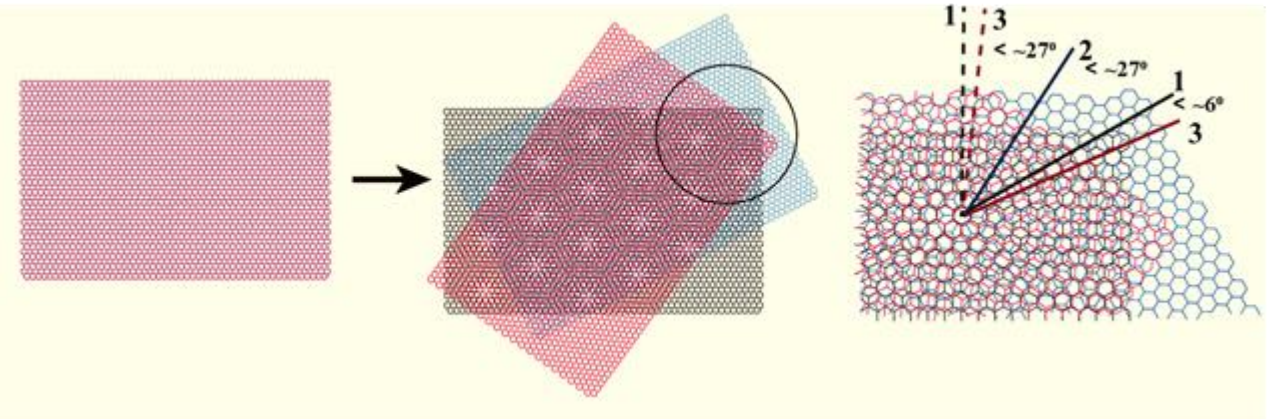

Fig. S10 Schematic representation of moiré patterns formed by three stacked sheets where sheets 1 and 2 forms an angle of 27º and 2 and 3 forms angle 27º, thus resulting in an angle of 6º for sheets 1 and 3.

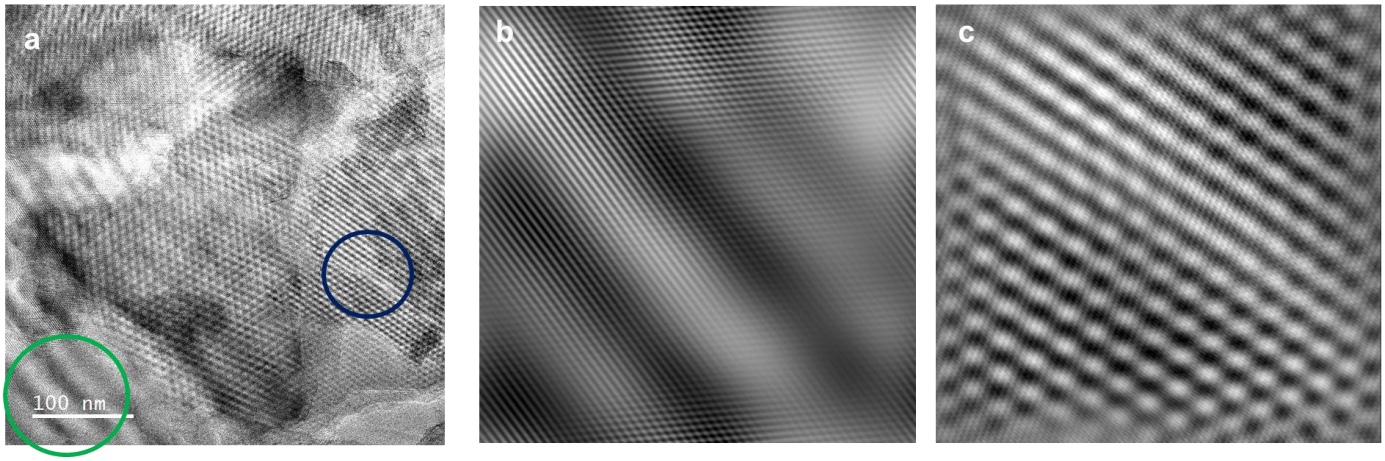

Fig. S11 (a) TEM image of a moiré superlattices. **(b)** IFFT of region circled in green in **a** and **(c)** IFFT of region circled in blue in **a**.

Determination of moiré periodicities

The moiré periodicities analyzed from Fig. S11b are - 24 nm, which is followed by 2.13 nm and 1.92 nm and the moiré periodicities from Fig. S11c are 6.61 nm, 2.36 nm and 1.06 nm. The corresponding angles for the above periodicities calculated from the equation

$$D = d/(2\mathrm{Sin}(\theta/2)) \qquad (6)$$

are 1.09º, 12.3º, 13.7º, 3.98, 11.1º and 25º respectively. In the above equation d is the lattice constant taken as 0.46 nm, D is the distance between moiré fringes and θ is the twist angle between two sheets. Further the angles obtained from the SAED between sheets 2 and 4 (1.3º), sheets 4 and 6 (11.7º), sheets 5 and 7 (4.3º) and 1 and 2 (25º) match well with the above calculated angles.

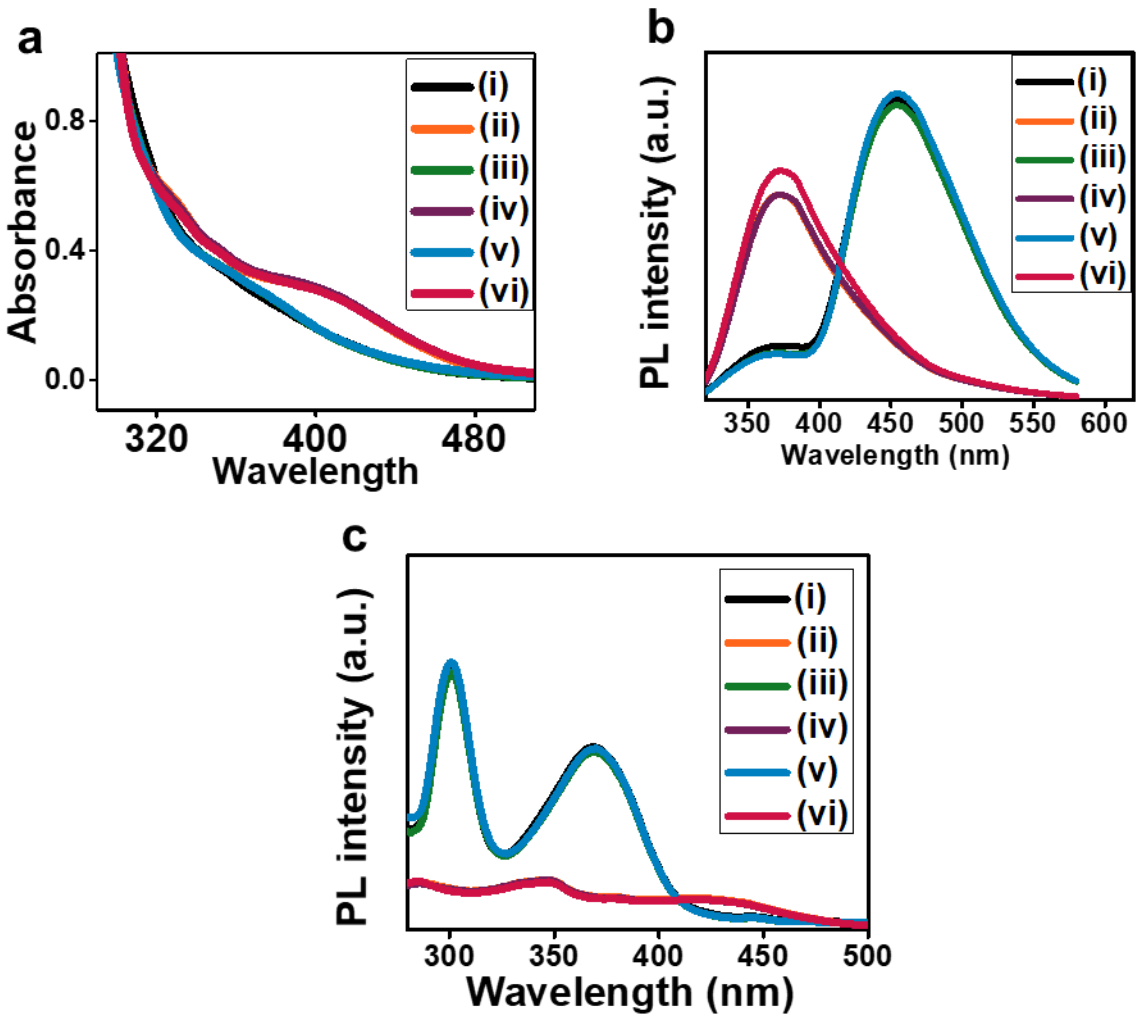

Fig. S12 Effect of alkali and acid. (a) Absorption spectra of trp solution after **(i)** 24 h of vigorous stirring at 80 °C (leading to the formation of trp moiré dispersion), which was subjected to a cycle of pH change where **(ii), (iii), (iv), (v)** and **(vi)** represent alternative addition cycles of 40 µL 1M NaOH and 40 µL 1M HCl solutions, respectively, to the mixture. **(B)** Photoluminiscence (PL) emission spectrum (λ_{ex} = 300 nm) of trp solution after **(i)** 24 h of vigorous stirring at 80 °(C) which is subjected to a cycle of pH change where **(ii), (iii), (iv), (v)** and **(vi)** represent alternative addition cycles of 40 µL 1M NaOH and 40 µL 1M HCl solutions, respectively, to the mixture. **(c)** PL excitation spectrum (λ_{em} = 452 nm) of trp solution after **(i)** 24 h of vigorous stirring at 80 °(C) which is subjected to a cycle of pH change where **(ii), (iii), (iv), (v)** and **(vi)** represent alternative addition cycles of 40 µL 1M NaOH and 40 µL 1M HCl solutions, respectively, to the mixture.

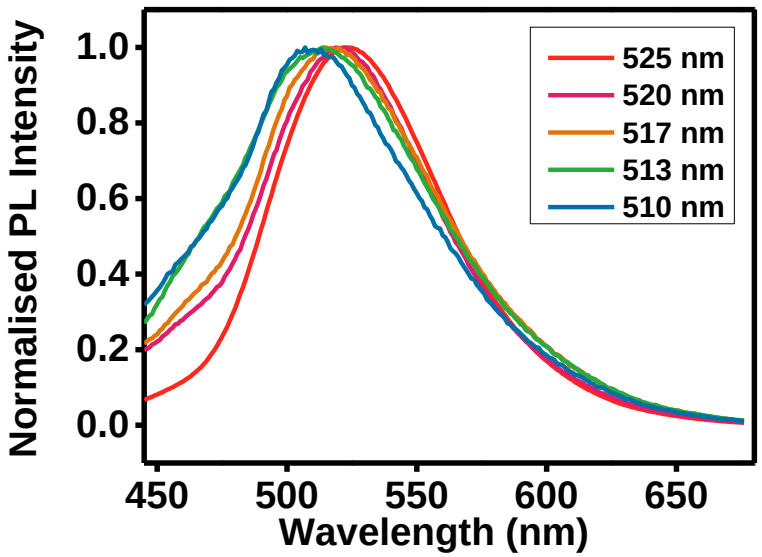

Fig. S13 Emission in the range 510-525 nm. Normalised PL emission (λ_{ex} = 425 nm) spectra of different experimental runs of trp (moiré) reaction after addition of alkali having peak maxima ranging from 510 nm to 535 nm.

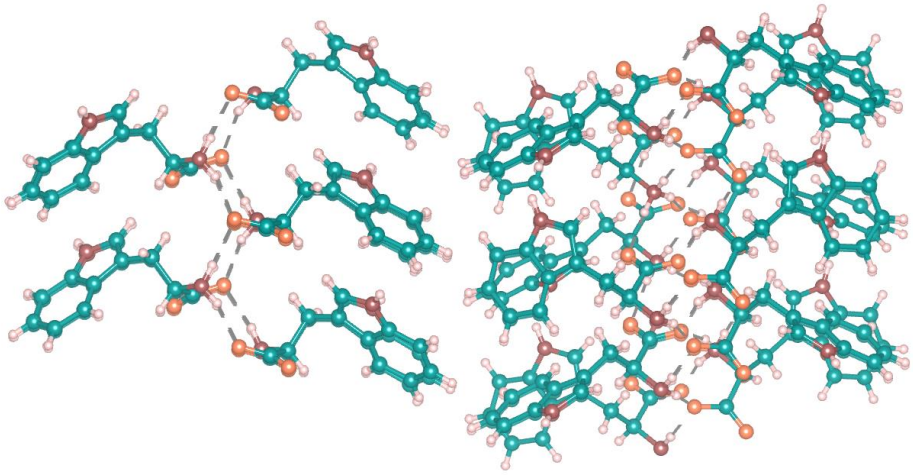

Fig. S14 Self-assembly of trp where the molecule assembles through alternate hydrogen bonding and hydrophobic interaction to form 2D supramolecular crystalline nanosheet.

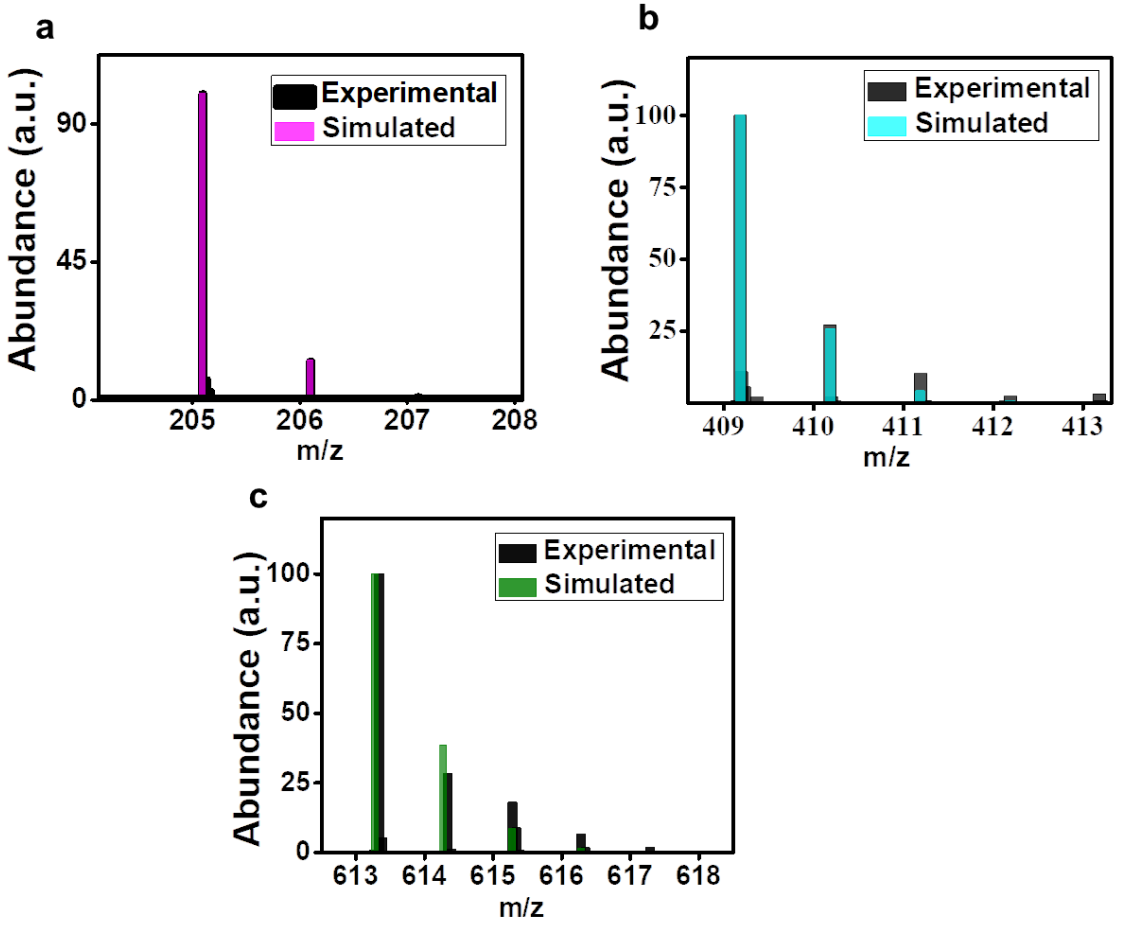

Fig. S15 ESI-MS of dispersion obtained after 2 h of reaction showing spectrum of **(a)** $[C_{11}H_{12}N_2O_2+1H^+]$ at m/z = 205.22; **(b)** $[(C_{11}H_{12}N_2O_2)_2 +1H^+]$ at m/z = 409.18 and **(c)** $[(C_{11}H_{12}N_2O_2)_3 +1H^+]$ at m/z = 613.17.

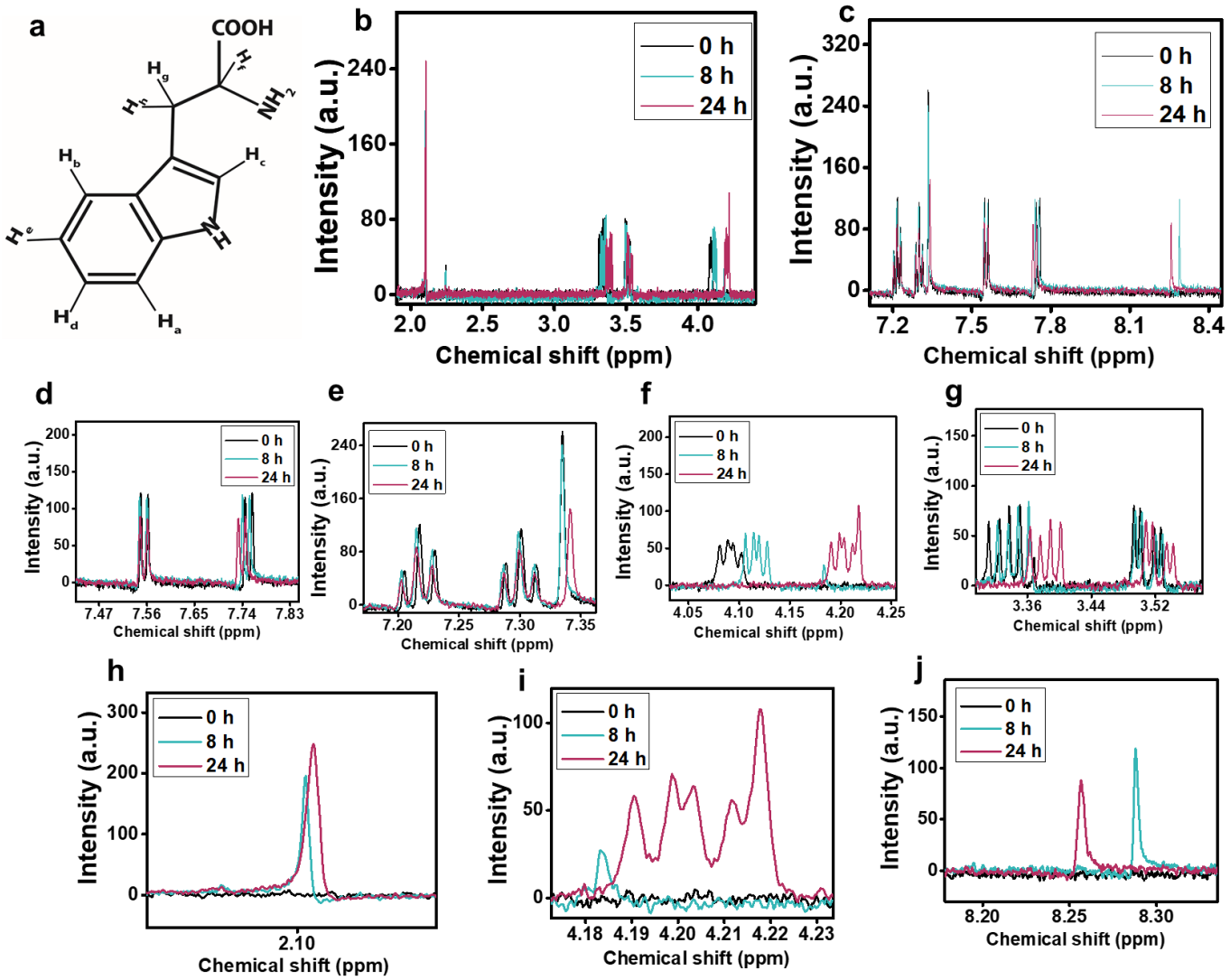

Fig. S16 ^{1}H NMR spectra of assembly of trp. Chemical shift of trp at different time intervals ranging from **(a)** Chemical structure of trp with different protons marked according to the chemical shift values**. (b)** 2-5 ppm. **(c)** 7-8.5 ppm. NMR spectrum of proton **(d)** H_a and H_b **(e)** H_e, H_d and H_c **(f)** H_f **(g)** H_g and H_h. New NMR peak observed at **(h)** 2.1 ppm (**i)** 4.2 ppm (**j)** 8.2 ppm.

Table S3. ^{1}H NMR peaks of trp solution in D_2O - leading to moiré superlattice formation - obtained at different times.

Chemical shift(ppm)/ Time (h)	H_a	H_b	H_c	H_d	H_e	H_f	H_g and H_h
0	7.75	7.55	7.33	7.3	7.21	4.09	3.42
8	7.75	7.55	7.33	7.29	7.21	4.11	3.42
24	7.74	7.55	7.34	7.29	7.21	4.2	3.45

Table S4. Integration ratio of aromatic protons and new peaks (H_x) relative to H_g at different times.

Integration ratio (Hx/Hg)/ Time (h)	H_a	H_b	H_c	H_d	H_e	Peak at 2.1 ppm	Peak at 4.2 ppm	Peak at 8.2 ppm
0	0.92	0.82	0.75	0.74	0.75	0	0	0
8	0.97	0.89	0.73	0.78	0.78	0.45	0.06	0.34
24	0.88	0.79	0.58	0.79	0.79	0.86	0.34	0.34

The moiré superlattices were formed by the twisted stacking of crystalline nanosheets at the crystal interfaces of hydrophobic region. The downfield and upfield shifts of the protons were caused due to self-assembly of trp. The integration ratio of the peaks with respect to H_g (which was taken as a standard for integration) suggested that with time there was a decrease in population of the aromatic protons. Among them the integration area of H_c decreased the most, indicating the change in chemical environment of the proton as the moiré superlattices

were continued to from. With time three new singlet peaks at 2.1, 4.2 and 8.3 ppm were observed along with the other ^{1}H NMR peaks of trp. A large chemical shift of H_c due to interaction at the crystal interface resulted in three new singlet peaks.

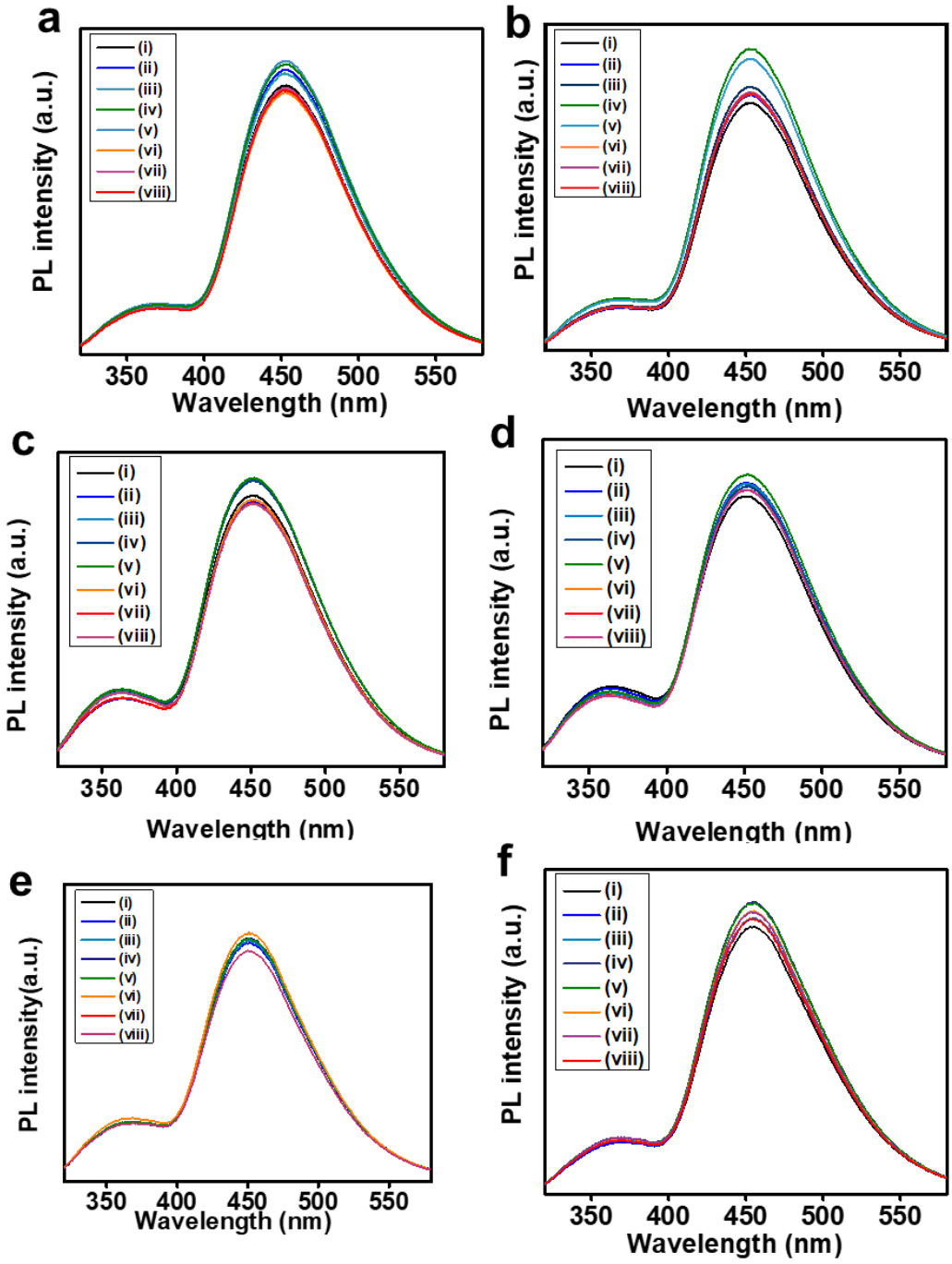

Fig. S17 Three different set of experiments for fluorometric CO_2 sensing and release measurements (a) PL spectra of the dispersion for experiment set 1 after **(i)** 24 h of reaction that was purged with CO_2 gas for **(ii)** 2 min, **(iii)** 5 min, **(iv)** 10 min and **(v)** 15 min, respectively and then kept in open for **(vi)** 5 min, **(vii)** 30 min **(viii)** 60 min respectively. **(b)**

PL spectra of the dispersion experiment set 1 after **(i)** 24 h of reaction that was purged with CO_2 gas for **(ii)** 2 min, **(iii)** 5 min, **(iv)** 10 min and **(v)** 15 min under the exposure of UV light and then kept in open for **(vi)** 5 min, **(vii)** 30 min **(viii)** 60 min respectively. **(c)** PL spectra of the dispersion for experiment set 2 after **(i)** 24 h of reaction that was purged with CO_2 gas for **(ii)** 2 min, **(iii)** 5 min, **(iv)** 10 min and **(v)** 15 min, respectively and then kept in open for **(vi)** 5 min, **(vii)** 30 min **(viii)** 60 min respectively. **(d)** PL spectra of the dispersion after **(i)** 24 h of reaction that was purged with CO_2 gas for **(ii)** 2 min, **(iii)** 5 min, **(iv)** 10 min and **(v)** 15 min under the exposure of UV light and then kept in open for **(vi)** 5 min, **(vii)** 30 min **(viii)** 60 min respectively. **(e)** PL spectra of the dispersion for experiment set 3 after **(i)** 24 h of reaction that was purged with CO_2 gas for **(ii)** 2 min, **(iii)** 5 min, **(iv)** 10 min and **(v)** 15 min, respectively and then kept in open for **(vi)** 5 min, **(vii)** 30 min **(viii)** 60 min respectively. **(f)** PL spectra of the dispersion experiment set 3 after **(i)** 24 h of reaction that was purged with CO_2 gas for **(ii)** 2 min, **(iii)** 5 min, **(iv)** 10 min and **(v)** 15 min under the exposure of UV light and then kept in open for **(vi)** 5 min, **(vii)** 30 min **(viii)** 60 min respectively.

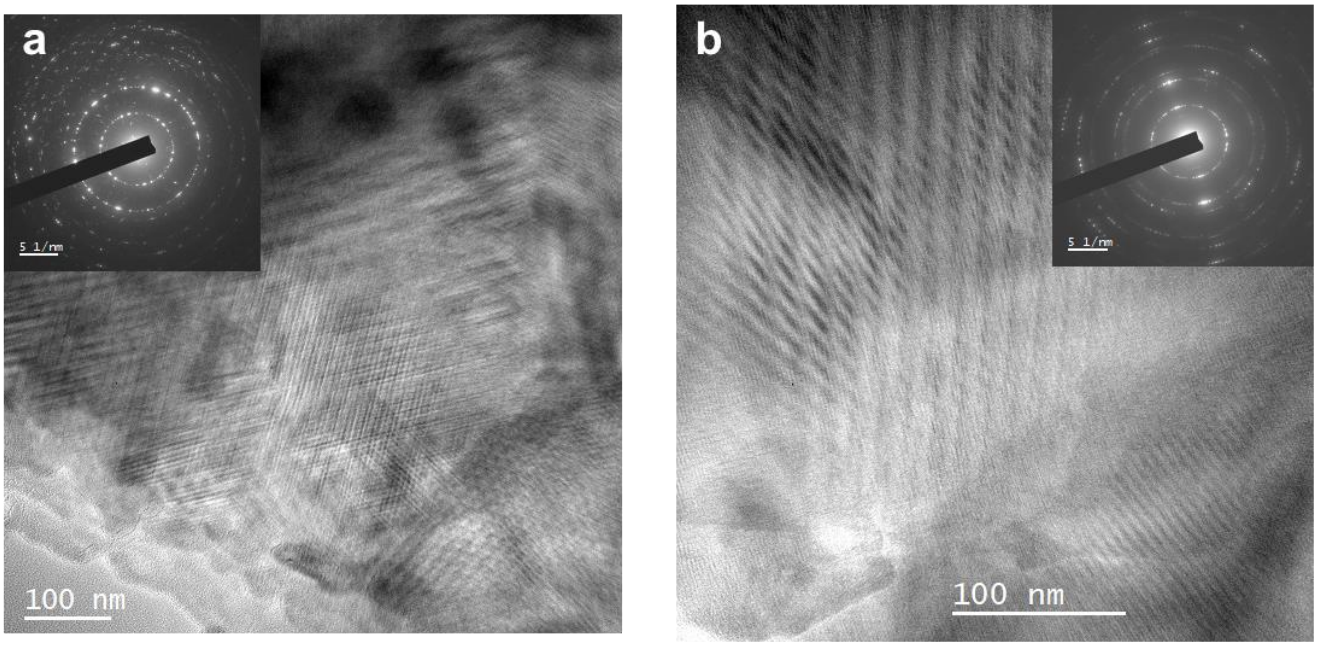

Fig. S18 TEM images of moiré superlattices of trp **(a)** before and **(b)** after CO_2 exposure in presence of UV irradiation. Inset: Corresponding SAED pattern.